A00-16779

AIAA 2000-0952

Sagnac Interferometry for Background Subtraction in Pump-Probe Spectroscopy

Kristen A. Peterson and Daniel J. Kane
Southwest Sciences, Inc.
Santa Fe, NM

38th Aerospace Sciences Meeting & Exhibit

10-13 January 2000 / Reno, NV

AIAA-2000-0952

SAGNAC INTERFEROMETRY FOR BACKGROUND SUBTRACTION IN PUMP-PROBE SPECTROSCOPY

Kristen A. Peterson* and Daniel J. Kane†
Southwest Sciences, Inc.
Santa Fe, New Mexico

ABSTRACT

We describe a novel pump-probe optical method, based on a Sagnac (anti-resonant ring) interferometer, which removes over 99% of the DC background light inherent in normal, two beam pump-probe measurements. Suppression of the DC component is critical for pump-probe imaging applications. In addition, this method greatly increases the signal-to-noise ratio compared with normal, two beam pump-probe measurements. The technique is demonstrated by detection of Rb atoms aspirated into a flame. The placement of the flame near the center of the ring interferometer reduces noise caused by flame turbulence.

INTRODUCTION

Techniques to image combustion species are important to the understanding of reactive flows. While experimental methods such as laser induced fluorescence remain the mainstay, much effort has been applied to the development of methods that are less sensitive to the collisional environment. Two techniques that have been investigated are polarization spectroscopy and pump-probe spectroscopy.

Polarization spectroscopy, for example, has been previously applied to line-of-sight measurements of several combustion species [1-4] and to two-dimensional imaging [4,5] in atmospheric pressure flames. Most flame polarization spectroscopy measurements have been made with ~10 ns or longer pulses. Thus, they are not collision free, but instead have emphasized the Doppler-free spectroscopic capabilities of this technique.

Time resolved polarization studies of OH radical in atmospheric pressure flames with ~ 40 ps time-resolution have been reported by Dreier and coworkers.[6,7] Those measurements show polarization relaxation times of ~300 ps for circular pump polarization and 500 - 700 ps for linear pump polarization, depending on the branch and line interrogated. The OH population lifetime (T_1) was measured by time resolved fluorescence as ~2 ns.

The principle disadvantage of polarization spectroscopy (as well as other DFWM and FWM techniques that measure dephasing) is that the signal can decay on a different timescale than the population decay rate because the signal is sensitive to collisionally induced dephasing. On the other hand, pump-probe spectroscopy measures different processes than does polarization spectroscopy. Pump-probe measurements, because they are sensitive to only T_1, or population decay, are thought to be less sensitive to collisions than are other $\chi^{(3)}$ methods.

In pump-probe spectroscopy, the pump beam is amplitude modulated (pulsed) and it is crossed with the probe in an absorbing sample. The pump modulation frequency is impressed on the resonant molecules. These molecules, in turn modulate the amplitude of the probe via absorption and stimulated emission. The amount of modulation is directly proportional to the number density of absorbers in the overlap region between the two beams. However, with normal pump-probe measurements, this modulation resides on a large DC background. Because of 1/f properties of noise sources, the DC background significantly increases noise and reduces the detection sensitivity. While lock-in detection can remove the DC background, restoring detection sensitivity, it is not easily applied to imaging systems. Thus, other means of DC removal are required.

One advantage of polarization spectroscopy over pump-probe spectroscopy is that the DC component of the probe beam is removed by crossed polarizers, making it more suitable for imaging applications. What is desirable is a

* Senior Research Scientist
† Senior Research Scientist

method of optical light subtraction that can be applied to pump-probe measurements that similarly removes the DC component. We show that this can be accomplished by using a Sagnac interferometer to provide interference between counter-propagating probe beams.

OPTICAL LIGHT SUBTRACTION

Our method incorporates a novel light canceling approach (demonstrated by Trebino and Hayden and which they call anti-resonant ring transient spectroscopy, or ARTS[8]) that involves sending the probe beam into a Sagnac (anti-resonant ring) interferometer. Operation of this interferometer can be understood by considering what happens to the probe pulse if it is directed into the optical system shown in Fig. 1. The probe first impinges on a 50/50 beam splitter. One part of the probe pulse travels around the ring in a clockwise direction – the other part of the probe pulse travels in the other direction. The two pulses travel exactly the same path and are then recombined at the same point on the 50-50 beam splitter; the two pulses interfere causing the forward traveling output from the ring to be essentially zero. The two pulses experience exactly the same distortions and exactly the same absorptions. In practice, about 0.01% of the light does leak out of the interferometer due to imperfections in the beam splitter. This leakage can be useful in improving the detection sensitivity by providing a local oscillator for homodyne detection.

If the counter propagating beams experience different optical losses, for example because of a time dependent absorption change induced in a sample placed off-center in the ring, the intensities of the two beams will not be equal at the beam splitter, and the leakage will increase. The pulse intensity from the Sagnac interferometer is given by[8]

$$I_{out} \propto 4\epsilon^2 + \epsilon\,\Delta\alpha(\tau)\,L + \left[\frac{1}{4}\Delta\alpha(\tau)\,L\right]^2 \qquad (1)$$

where ϵ is the deviation in beam splitter reflectivity from 0.5 (*i.e.* the leakage), $\Delta\alpha(\tau)$ is the pump induced change in absorption and L is the sample length. The first term in the equation above is the beam-splitter leakage and the third term is the transient absorption. The second term is the homodyned signal arising from the interaction between the leakage field and the transient absorption signal field. Assuming laser shot noise is the dominant noise source, the signal-to-noise improvement over pump-probe spectroscopy is[8]

$$\frac{SNR_{ARTS}}{SNR_{pump-probe}} = \frac{1}{4\epsilon}. \qquad (2)$$

Suppose we place a flame inside the ring at or near the ring center (see "Sample" in Fig. 1). Now suppose we excite a species in the flame, at a position slightly counter-clockwise of ring center, with a short pump pulse a few picoseconds long, just as the clockwise pulse impinges on the sample. The counter-clockwise pulse reaches the excited point before the pump pulse, while the clockwise pulse arrives after the pump pulse. This will causes the intensities of the two counter-propagating probe pulses to be different and an output leakage pulse will result. This leakage signal can be monitored by a single-element detector or imaged with a CCD camera.

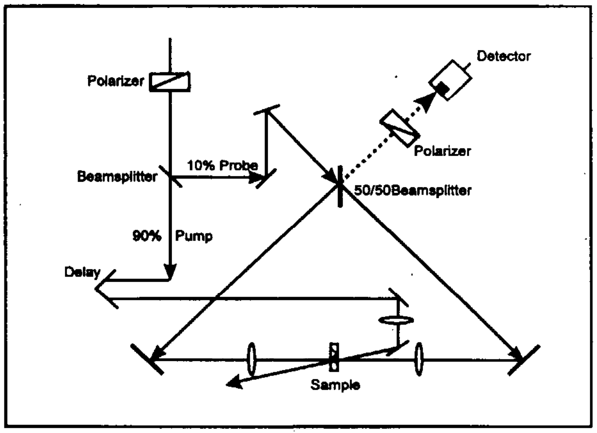

Figure 1 Schematic of the anti-resonant ring pump-probe apparatus.

The population decay can be obtained by delaying the pump-pulse so that it arrives at various times before and after the clockwise pulse, but such that it always arrives after the counter-clockwise pulse. In this configuration the counter-clockwise pulse always probes the sample in the un-excited state. How much of the decay can be obtained depends on the decay time constant and the position of the sample in the ring, since the sample position affects the time separation between the two counter-propagating probe pulses.

INTERFEROMETER CONSTRUCTION

A Sagnac interferometer was constructed for use with a mode-locked Ti:sapphire laser in order to test the utility of anti-resonant ring transient spectroscopy (ARTS) for DC background cancellation and for use in pump-probe imaging of flame species. The Ti:sapphire laser is a Clark-MXR Instruments model NJA-5, which is mode locked at 100 MHz, has pulse widths of ~ 100 fs and average power of 300-400 mW. The Ti:sapphire laser is pumped by a Spectra Physics Millennia V frequency doubled, diode pumped $Nd:YVO_4$ laser.

A diagram of the interferometer is shown in Fig. 1. A reflective neutral density filter (effective OD = 1.0) is used as a beam splitter to provide 10% of the laser beam to the interferometer. The remainder is directed to an optical delay line for use as a pump beam. The probe beam is divided into two equal beams by a 50/50 beam splitter. The ring dimensions, for a 45 degree incident angle on the beam splitter, are 64.8 cm between beam splitter and mirrors and 91.4 cm between the two mirrors. This corresponds to an optical path of 7.3 ns.

To reduce vibration sensitivity, the interferometer optics are mounted on sturdy, one inch diameter posts which are mounted on a vibrationally damped and tuned breadboard.

One difficulty with this optical arrangement is that a well-aligned and nulled ring reflects a backwards propagating beam into the laser. This causes the Ti:sapphire laser to stop mode-locking. When the full ring output is detected without spectral filtering, the intensity at the detector is high enough that a neutral density filter can be placed before the ring input and the back-reflected beam is sufficiently attenuated to prevent feedback into the mode-locked Ti:sapphire laser. However, when the ring output is spectrally filtered through a monochromator, as for the rubidium measurements presented below, the full probe beam must be input into the ring in order to have enough intensity at the detector. In this case a Faraday optical isolator is placed in the laser beam. The isolator is highly dispersive and lengthens the femtosecond laser pulses to several picoseconds (without reducing the spectral width). This pulse lengthening effect can be seen in the data presented below, but will not be an issue if tens of picoseconds long pulses are used for picosecond pump-probe imaging applications.

Lenses may also be added inside the ring to focus or expand the beam into the sample. For the pump-probe point measurements, two 20 cm focal length lenses separated by 40 cm are used. With no lenses, the beam diameter is ~ 1 mm.

Depolarization of the beams by optics in the ring can degrade the interferometer performance. The interferometer performs best when the polarization of the input beam is highly linear and is matched to the reflection characteristics of the beam splitter and reflective optics. We used mirrors and a beam splitter designed for s-polarized light (polarization perpendicular to the horizontal reflection plane). A polarizer was placed in the input beam to ensure that the input beam was well polarized. To ensure that any depolarization caused by optics was not detected, a polarizer, set parallel to the input polarizer, was placed in the ring output beam before the detector. Using the polarizers in this manner improved the ring's extinction ratio (reduced the leakage) by a factor of 2.

The extinction ratio of the interferometer is critically dependent on optical alignment. In order to make fine alignment adjustments, the beam splitter is in a gimbal mount controlled by two motorized micrometers (Oriel Corp.) for fine horizontal and vertical aiming. The beam splitter mount is bolted on top of a translation stage equipped with a finely adjustable micrometer. Translation is perpendicular to the beam splitter surface. This combination of the gimbal mount and translation stage provides complete control over alignment of the beam splitter angle and position and provides the fine adjustment necessary to optimize the ring alignment..

The extinction ratio is optimized by making small changes in the ring geometry to change the angle of incidence on the beam splitter. The best extinction ratio, δ, (defined as the ratio of the leakage power to the ring input power) achieved with this interferometer is 5×10^{-4}. This occurs at an incident angle of 45.6 degrees. Since $\delta = 4\epsilon^2$, eq. 2 predicts a signal-to-noise improvement of 22 over two beam pump-probe. This extinction ratio implies a beam splitter reflectivity of 0.51 (ϵ = 0.01), assuming there is no other noise source than laser noise.

We expect with a highly coherent, monochromatic beam that extinction near 10^{-6} is achievable.[8] We observed that when the laser is tuned to a different center wavelength, it is necessary to re-optimize the ring geometry for best extinction. For example, after optimization at 780 nm, tuning the laser to 760 nm increases the leakage by a factor of 3. This illustrates one factor that is limiting our ability to null the output beam in this system. The sub-picosecond Ti:sapphire laser has a spectral bandwidth (full width at half maximum) of 10 to 15 nm – depending on laser adjustment and pulse width. Because of this large bandwidth, the beam splitter cannot be optimized simultaneously for all wavelengths within a laser pulse. Better nulling is expected when picosecond pulses are used. For example, a Fourier transform limited 10 ps pulse at 780 nm has a spectral bandwidth of only 0.1 nm.

EXPERIMENTAL RESULTS

The setup can be easily changed from the ARTS configuration to a two beam pump-probe (2BPP) configuration by simply mis-aligning the ring with the beam splitter horizontal adjustment so that the counter-clockwise traveling beam is blocked by one of the alignment irises. In this way, comparisons between ARTS and 2BPP are easily made without changing optics or pump and probe beam overlap. The ring output (or clockwise propagating beam for 2BPP) is directed to a single element photodiode for point measurements. The detector output is sent to a lock-in amplifier and the lock-in output to a computer, which controls the delay line and data acquisition. The pump beam is modulated near 1 kHz using an optical chopper which also provides the reference frequency for the lock-in amplifier. The S/N enhancement for ARTS measurements over 2BPP measurements was first evaluated using a 780 nm long pass Schott Glass filter as the sample.

When using a lock-in amplifier, valid comparisons can be made only if the lock-in filters and time constant, and the scan parameters and number of scans averaged are the same in each case. It is also important that the magnitude of the DC component removed by the lock-in is similar in both case. Furthermore, there is very little light on the detector when the interferometer is nulled, thus detector noise can contribute to the S/N in that case and not for 2BPP measurements unless care is taken to match the light levels for the different measurements. A variable neutral density filter before the detector was used to match the light intensity on the detector when directly comparing ARTS and 2BPP measurements. (Of course, for imaging experiments with ARTS, a lock-in will not be used. But, for these point measurements, ARTS signals were observable without a lock-in and 2BPP signals were not, making a lock-in necessary for these comparison measurements.)

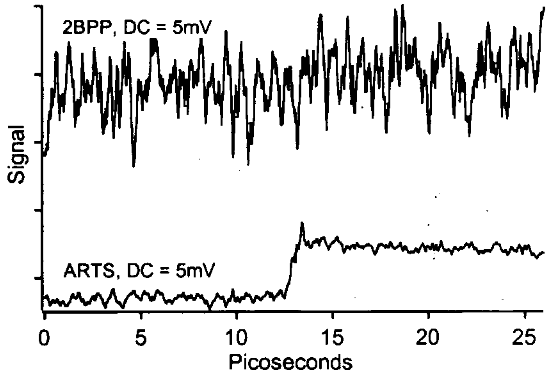

Figure 2 Comparison of ARTS and 2BPP scans with equal DC background levels. The sample is a 780 nm long pass filter. The ARTS extinction ratio is 1.5×10^{-3} and the S/N enhancement is 13.

Figure 2 shows an ARTS scan using an extinction ratio of 1.5×10^{-3} compared with an equivalent 2BPP scan. The S/N for the ARTS measurement is 13 and that for the 2BPP measurement is 1. S/N for these scans is defined as the difference between the average signal level before and after time zero divided by the standard deviation of the signal before time zero. The observed S/N enhancement is in excellent agreement with theoretical predictions. From equation 3, the S/N enhancement expected for $\delta = 1.5 \times 10^{-3}$ is 12.9. This enhancement allows observation of details in the ARTS scan that are not seen in the 2BPP scan. At time zero, when the pump and probe beams are temporally overlapped, a coherent scattering spike can be seen clearly in the ARTS data, but is obscured by noise in the 2BPP data.

The performance of the interferometer for combustion measurements was tested by making point measurements on rubidium in a flame. Rubidium chloride (100 mg/mL aqueous solution) was aspirated into an atomic absorption burner with methane and air flowed at a stoichiometric ratio. Sixty percent of the total air flow was directed to the aspirator. The flame was placed in the center of the ring, *i.e.* exactly opposite the beam splitter with the beam crossing slightly off center.

When the flame is lit, slight adjustments to the optical alignment using the beam splitter are necessary to optimize the extinction ratio. This is because of thermal deflection effects. The *average* extinction ratio is the same for flame on or flame off; however, there are greater, long-time (~1 Hz) fluctuations in the leakage beam when the flame is on. The noise in the leakage beam when the flame is at ring center is about a factor of five greater than when the flame is off. If the flame is moved 2 inches away from the ring center, the noise increases by a factor of 2. However, the data we present below shows that additional noise caused by the flame is present in both the ARTS and 2BPP measurements and most of the signal-to-noise improvement for ARTS over 2BPP is maintained for flame measurements.

The laser was tuned so its center wavelength was near 780 nm. Atomic Rb absorption lines are narrow, less than 0.1 cm^{-1} at atmospheric pressure and 2000 K. To have any hope of observing pump-probe signals using the spectrally broad femtosecond Ti:sapphire pulses, it is necessary to spectrally filter the probe beam. Spectral filtering will not be necessary when 10 picosecond or longer pulses are used. A 1/4 meter monochromator and appropriate optics to match the monochromator f-number were used in the ring output beam for this purpose. The monochromator was calibrated with Rb and Ne lamps. The photodiode detector was placed at the exit slit and its output sent through a lock-in amplifier and then to a computer.

Figure 3 shows a spectrum of the Rb line in the flame, using a high Rb concentration, obtained by scanning the monochromator while sending the laser beam through the monochromator with the slits at 20 μm. The broad, gaussian baseline is the laser pulse spectrum.

Figure 4 shows ARTS and 2BPP data for the 780.03 nm Rb line. The concentration of the aspirated Rb solution is the same for both the ARTS and 2BPP measurements. For both techniques, scans are also shown for flames without Rb. The interferometer extinction ratio is 1.5 × 10^{-3} and the slits are set to 30 μm (~2 cm^{-1} resolution). The observed S/N enhancement is 7 while the predicted enhancement is 13. The long rise times in the ARTS and 2BBP scans are due to the long pulses caused by dispersion in the Faraday isolator, as discussed above.

Figure 3 Spectrum of Rb aspirated into a flame obtained by using the spectrally broad Ti:sapphire laser beam and a scanning monochromator.

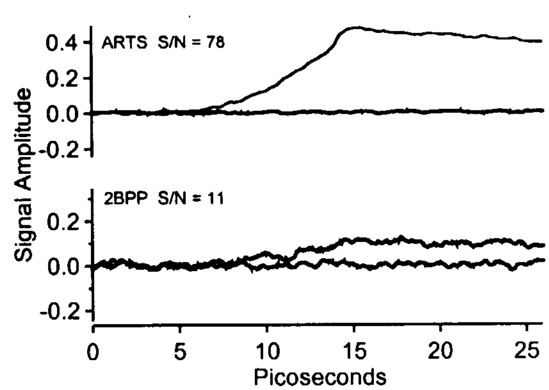

Figure 4 Comparison of ARTS and 2BPP scans for Rb aspirated into a flame. Also shown are scans with no Rb in the flame. ARTS provides a S/N enhancement of 7 over 2BPP in the flame.

Despite a factor of 2 decrease in performance when the flame is present, the interferometer still provides a significant improvement in signal-to-noise over 2BPP and it allows suppression of the DC component of the signal – which is crucial for imaging experiments.

CONCLUSIONS

We found that even in the presence of a flame, ARTS can easily and routinely increase the signal-to-noise ratio by a factor of 10 for wide bandwidth pulses. Factors of 50 to 100 are expected with narrower bandwidths, because of improved beamsplitter performance, and with improved optics. Furthermore, this technique suppresses > 99% of the DC probe beam, making two-dimensional pump-probe imaging of flame species feasible.

ACKNOWLEDGMENTS

This work was funded by DOD AFOSR contract #F33615-96

REFERENCES

1. Nyholm, K.; Maier, R.; Aminoff, C. G.; Kaivola, M. *Applied Optics* **1993**, *32*, 919-924.

2. Nyholm, K.; Kaivola, M.; Aminoff, C. G. *Applied Physics B* **1995**, *60*, 5-10.
3. Lofstedt, B.; Fritzon, R.; Alden, M. *Applied Optics* **1996**, *35*, 2140-2146.
4. Lofstedt, B.; Alden, M. *Optics Communications* **1996**, *124*, 251-257.
5. Nyholm, K.; Fritzon, R.; Alden, M. *Optics Letters* **1993**, *18*, 1672-1674.
6. Dreizler, A.; Tadday, R.; Suvernev, A. A.; Himmelhaus, M.; Dreier, T.; Foggi, P. *Chemical Physics Letters* **1995**, *240*, 315-323.
7. Suvernev, A. A.; Taddy, R.; Dreier, T. *Physical Review A* **1998**, *58*, 4102-4115.
8. Trebino, R.; Hayden, C. C. *Optics Letters* **1991**, *16*, 493.